Acta Crystallographica Section D
Biological Crystallography
ISSN 0907-4449

Wavelet analysis of electron-density maps

Peter Main[a] and Julie Wilson[b]*

[a]Department of Physics, University of York, Heslington, York YO10 5DD, England, and [b]Department of Chemistry, University of York, Heslington, York YO10 5DD, England

Correspondence e-mail: julie@ysbl.york.ac.uk

Received 11 August 1999
Accepted 28 February 2000

The wavelet transform is a powerful technique in signal processing and image analysis and it is shown here that wavelet analysis of low-resolution electron-density maps has the potential to increase their resolution. Like Fourier analysis, wavelet analysis expresses the image (electron density) in terms of a set of orthogonal functions. In the case of the Fourier transform, these functions are sines and cosines and each one contributes to the whole of the image. In contrast, the wavelet functions (simply called wavelets) can be quite localized and may only contribute to a small part of the image. This gives control over the amount of detail added to the map as the resolution increases. The mathematical details are outlined and an algorithm which achieves a resolution increase from 10 to 7 Å using a knowledge of the wavelet-coefficient histograms, electron-density histogram and the observed structure amplitudes is described. These histograms are calculated from the electron density of known structures, but it seems likely that the histograms can be predicted, just as electron-density histograms are at high resolution. The results show that the wavelet coefficients contain the information necessary to increase the resolution of electron-density maps.

1. Introduction

One of the important goals of current crystal structure analysis is to develop methods for the complete *ab initio* determination of macromolecular structures. A number of different approaches are being made towards this problem and there is evidence of progress. One course of action, which has grown out of the work carried out at York, is to

(i) determine an initial image of the molecule at about 10 or 15 Å resolution to show the molecular envelope,

(ii) increase the resolution of this image to about 5 Å to resolve the tertiary structure and

(iii) use image-processing techniques to improve the electron-density map and to increase its resolution to that of the X-ray data.

The easiest of these stages and hence the first one to be substantially developed is (iii) above. It was started by Zhang & Main (1990), who produced the computer program *SQUASH*, and continued by Cowtan & Main (1993). This has resulted in the current computer program *DM* in the *CCP*4 protein crystallography program library (Collaborative Computational Project, Number 4, 1994). In the absence of *ab initio* images, it has been very successful at improving the electron-density maps obtained by more standard methods such as molecular replacement, multiple isomorphous replacement and especially multiple-wavelength anomalous

dispersion. Its success depends upon having a starting image with a resolved tertiary structure and so is limited to resolutions higher than about 5 Å.

Stage (i) above is currently being developed by a number of people (see, for example, Lunin *et al.*, 1990). It typically yields images of between 10 and 15 Å resolution, depending upon the volume of the asymmetric unit and the solvent content. Higher resolutions than this are currently not available because the only information used by the method is the electron-density histogram, the solvent content and the observed diffraction pattern. This is sufficient to yield the molecular envelope, but no structural details within the molecule.

There is evidently a resolution gap between about 12 and 5 Å in which it is difficult to determine phases reliably using only the X-ray data from a single diffraction pattern. Development of a method to achieve this would make possible the complete *ab initio* determination of the crystal structure. This is the task of stage (ii) above and it has proved to be an extremely difficult problem. This paper describes some recent work which may go some way towards solving the problems involved.

2. Wavelet analysis

Wavelet analysis has become a highly successful technique in a number of fields, notably in signal and image processing, and there is now an abundance of literature on the subject. For completeness, we give a brief outline of the relevent theory here.

As we are dealing with electron density defined at grid points, we only consider the discrete wavelet transform (DWT) and use the multi-resolution approach developed by Mallat (1989). We consider first the case of one-dimensional electron density and then show that the theory easily extends to three dimensions.

We consider a function $\varphi(x)$, which together with its integer translates forms an orthonormal basis for L_2 (R) and therefore for the type of function that we are interested in, *i.e.* the electron density. We can then represent the electron density $\rho(x)$ as a linear combination of these functions

$$\rho(x) = \sum_{k=1}^{n} A_k \varphi(x-k), \tag{1}$$

where n is the number of grid points. As we only consider $\rho(x)$ at discrete grid points, $x = 1, \ldots, n$, the parameter k translates φ by an integer number of grid points. We use the variable x rather than one which conventionally denotes an integer as the theory extends to a real-valued variable, whereas k will always be an integer. Since the functions $\{\varphi(x-k), k = 1, \ldots, n\}$ are orthonormal, the coefficients A_k are just the inner products $\langle \rho(x), \varphi(x-k) \rangle$ and so can easily be calculated (for example, in the wavelet context, see note 12, p. 166, Daubechies, 1992). Thus, we have

$$\rho(x) = \sum_{k=1}^{n} \langle \rho(x), \varphi(x-k) \rangle \varphi(x-k). \tag{2}$$

In the familiar Fourier representation of the electron density as a sum of structure factors, the orthogonal functions are sines and cosines and each one contributes to every part of the density. In direct contrast, we choose our function $\varphi(x)$ to have compact support, *i.e.* one which is only non-zero for a small number of grid points, so that each of the translates only contributes to a particular part of the electron density. [Obviously, the function $\varphi(x)$ must be periodic with period n the same as the electron density, but we only consider one period here.] In addition, we require a relationship between the functions $\varphi(x-k)$ and the same functions scaled by a factor of two. This is achieved by choosing $\varphi(x)$ such that it satisfies a scaling equation

$$\varphi(x/2) = \sum_{k=1}^{n} C_k \varphi(x-k) \tag{3}$$

for some coefficients C_k. Provided n is a multiple of 2, these wider functions can be used to give an approximate or 'smoother' version of the electron density requiring only half as many coefficients,

$$\rho(x) \simeq \sum_{k=1}^{n} \langle \rho(x), \varphi(x/2-k) \rangle \varphi(x/2-k). \tag{4}$$

We store the differences between the exact representation of the electron density in (1) and the approximation in (4) in terms of a related function, $\psi(x)$, defined such that

$$\psi(x/2) = \sum_{k=1}^{n} D_k \varphi(x-k), \tag{5}$$

where it can be shown that the coefficients D_k are related to the C_k in (3) by

$$D_k = (-1)^{n-k} C_k.$$

Using these functions, we can again express the electron density exactly, but this time as the smoothed version in (4) plus the details which need to be added to this,

$$\rho(x) = \sum_{k=1}^{n/2} \langle \rho(x), \varphi(x/2-k) \rangle \varphi(x/2-k) + \sum_{k=1}^{n/2} \langle \rho(x), \psi(x/2-k) \rangle \psi(x/2-k). \tag{6}$$

Notice that, in going from (1) to (4), the number of coefficients required is not increased. If n is also a multiple of 4, we can repeat the process on the smoothed density to obtain an even smoother version plus two different levels of detail, again without increasing the number of coefficients. Thus, we can write

$$\rho(x) = \sum_{k=1}^{n/4} \langle \rho(x), \varphi(x/4-k) \rangle \varphi(x/4-k) + \sum_{n=1}^{n/4} \langle \rho(x), \psi(x/4-k) \rangle \psi(x/4-k) + \sum_{n=1}^{n/2} \langle \rho(x), \psi(x/2-k) \rangle \psi(x/2-k) \tag{7}$$

and, provided n is a power of 2, we can keep repeating the process, always saving the details from the previous levels and

smoothing further to separate out a new level of detail. If, say, $n = 2^r$, we would eventually arrive at a situation with a single φ function representing the smooth component and r different levels of detail, giving the full wavelet transform of the electron density, $\rho(x)$. The function φ is referred to as the smoothing function or, because of (3), the scaling function, whereas the functions ψ, which encode the details, are called the wavelet functions or simply wavelets.

The wavelet coefficients $\langle \rho(x), \varphi(x/2^r - k)\rangle$ and $\langle \rho(x), \psi(x/2^r - k)\rangle$ tell us how much each of the scaling functions $\varphi(x/2^r - k)$ and the wavelet functions $\psi(x/2^r - k)$ contribute to the electron density. The dilation parameter 2^r gives the level of detail and the translation parameter k gives the position in the map that a particular function occurs. The scaling equation (3) gives a relationship between the coefficients in (2) and those in (4) since

$$\begin{aligned}\langle \rho(x), \varphi(x/2 - k)\rangle &= \int \rho(x)\varphi(x/2 - k)\,\mathrm{d}x \\ &= \int \rho(x) \sum_{j=1}^{n} C_j \varphi(x - 2k - j)\,\mathrm{d}x \\ &= \sum_{j=1}^{n} C_j \int \rho(x)\varphi(x - 2k - j)\,\mathrm{d}x \\ &= \sum_{j=1}^{n} C_{j-2k} \langle \rho(x)\varphi(x - j)\rangle \qquad (8)\end{aligned}$$

and similarly, using (5), we find that

$$\langle \rho(x), \psi(x/2 - k)\rangle = \sum_{j=1}^{n} D_{j-2k} \langle \rho(x), \varphi(x - j)\rangle, \qquad (9)$$

so that the coefficients in (6) can be obtained from those in (2). Thus, the coefficients at each level of the transform can be calculated from those of the previous level, allowing the wavelet transform to be calculated quickly and easily, and as the wavelet coefficients completely characterize the electron density, only these need to be stored. This is the basis for the fast wavelet transform (FWT) which can be implemented by matrix methods (see Press *et al.*, 1992). However, it should be noted that in Press *et al.* (1992) the matrix is applied directly to a function $f(x)$ rather than the initial coefficients, $\langle f(x), \varphi(x - k)\rangle$. Strictly speaking this is incorrect, although it is a common practice where $f(x)$ is considered an approximation to the coefficients $\langle f(x), \varphi(x - k)\rangle$. The effect of this approximation depends on the particular application, but some argue that it should never be performed and Strang & Nguyen (1996) refer to this as a 'wavelet crime'.

At any level of the wavelet transform, the electron density can be restored by multiplying the wavelet coefficients by the corresponding wavelet functions, providing of course that the coefficients were calculated from correct starting coefficients $\langle \rho(x), \varphi(x - k)\rangle$ and not from the approximation $\rho(x)$. However, the orthogonality of the functions also allows a simple inverse transform to be performed.

In two dimensions, the smoothing function can be defined by

$$\varphi(x, y) = \varphi(x)\varphi(y),$$

leading to the wavelet functions

$$\begin{aligned}\psi_1(x, y) &= \varphi(x)\psi(y), \\ \psi_2(x, y) &= \psi(x)\varphi(y), \\ \psi_3(x, y) &= \psi(x)\psi(y)\end{aligned}$$

for the first level of the transform. Similarly, in three dimensions, the smoothing function $\varphi(x, y, z) = \varphi(x)\varphi(y)\varphi(z)$ gives seven different wavelet functions for a single level transform, though these can be grouped together into three types depending on the number of ψ functions involved.

A set of wavelet functions is defined by the wavelet filter coefficients $\{C_k, k = 1, \ldots, m\}$, where m is the support of the wavelet, *i.e.* the number of non-zero integer values of φ. [Note that if $m < n$, which is usual, some of the coefficients C_k in (3) and hence the coefficients D_k in (5) will be zero.] There are many wavelet systems which have been purpose-built to satisfy the requirements on the functions φ and ψ set out in the above discussion. However, the wavelets constructed by Daubechies (1992) have particularly good compact support and, as we are dealing with a relatively small number of grid points, are particularly suitable for our purpose. Daubechies' wavelets may have 2, 4, 6, ... filter coefficients and cannot be

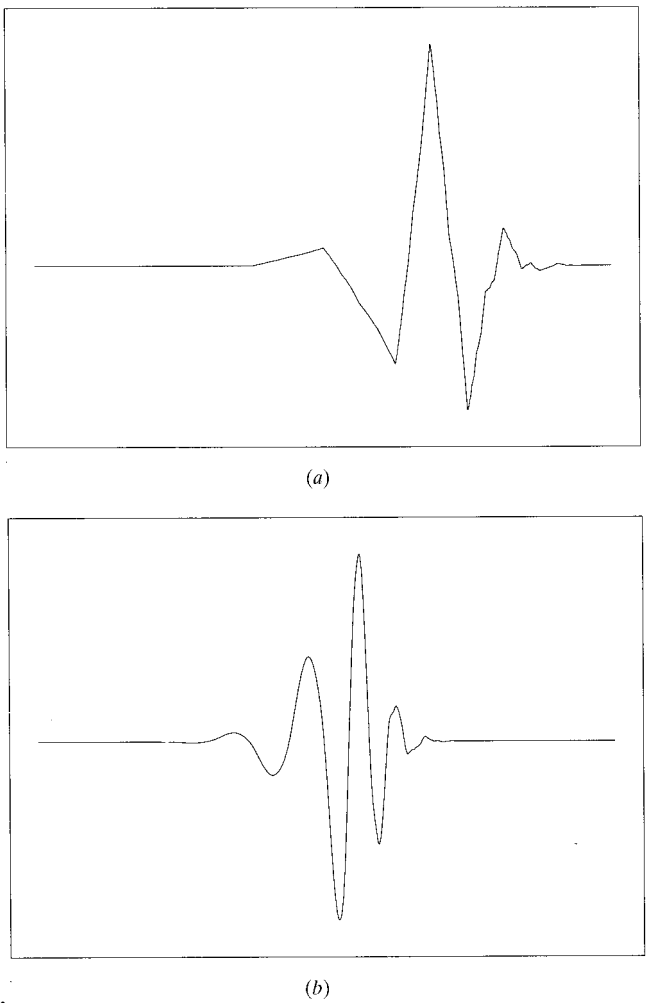

Figure 1
A single wavelet function from the Daubechies' family of order 6 (*a*) and of order 20 (*b*).

expressed as analytical formulae but are instead formed by an iterative procedure *via* (3). Performing an inverse wavelet transform on a unit vector shows what the wavelet functions actually look like. Fig. 1 shows a single wavelet function for Daubechies' wavelet of order 6, *i.e.* the wavelet constructed from six filter coefficients, and for Daubechies' wavelet of order 20. An orthonormal basis consists of scalings and translations of either of these functions. As we have said, the relationships in (8) and (9) mean that in the implementation of the FWT we only need to know the filter coefficients $\{C_k,\ k = 1,\ \ldots,\ m\}$ and Daubechies has tabulated these for wavelets of order up to 20, some of which are also available in Press *et al.* (1992).

3. Image analysis

The problem of increasing the resolution of a low-resolution electron-density map is one of adding the right sort of detail to it and in the right place. Since wavelet analysis separates an image into smooth and detail components, it affords the possibility of controlling or even creating the detail to be added to the map. Rather than use a complete wavelet transform, only a single stage has been used in this analysis. For a two-dimensional image, the transform is performed by transforming the x and y directions separately. The x transform separates the image into the smooth half and the detail half, as illustrated in Fig. 2. This is followed by the y transform, which produces the four areas at the right of the figure. There are thus four kinds of wavelet coefficients – the coefficients of the smoothing functions, $\varphi(x - j, y - k)$, which we denote by SS, and the coefficients of the three different wavelet functions, $\psi_1(x - j, y - k)$, $\psi_2(x - j, y - k)$ and $\psi_3(x - j, y - k)$, denoted SD, DS and DD, respectively. Now $\psi_1(x - j, y - k) = \varphi(x - j)\psi(y - k) = \psi(y - k)\varphi(x - j)$ and $\psi_2(x - j, y - k) = \psi(x - j)\varphi(y - k) = \varphi(y - k)\psi(x - j)$ so that, if we do not expect systematic differences between the x and y directions, the SD and DS coefficients cannot be distinguished statistically. For a two-dimensional image, we thus have three classes of wavelet coefficients. For a three-dimensional image, one-dimensional wavelet transforms are performed in the three different directions giving SSS, SSD, SDS, DSS, SDD, DSD, DDS and DDD coefficients. Of these, the SSD, SDS and DSS coefficients will be indistinguishable, as will the SDD, DSD and DDS. There will therefore be four classes of wavelet coefficients.

The immediate questions arising are

(*a*) is the expected detail in the image reflected in the statistical distribution of the coefficient values?

(*b*) Can the wavelet-coefficient histograms be predicted for an unknown image?

(*c*) Can the image be constructed from the histograms of its wavelet coefficients?

Some progress has been made towards answering these questions.

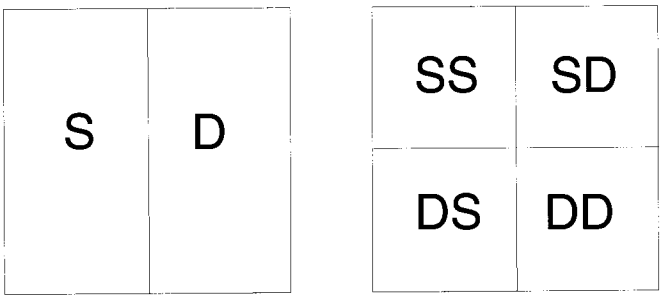

Figure 2
The division of a two-dimensional image after one stage of a wavelet row transform followed by a column transform. S = smooth, D = detail.

4. Histograms

The four different wavelet-coefficient histograms considered were the SSS, SSD (which includes the SDS and DSS coefficients), SDD (including the DSD and DDS coefficients) and the DDD. They were accumulated for a number of maps of different structures at different resolutions and grid sizes. Different sizes of molecule and solvent content were also used. The four histograms are quite distinct, but each has a shape which appears to be independent of both the structure and the grid size. In addition, only the SSS histogram has a shape which depends upon resolution. Examples are shown in Fig. 3.

The SSS histogram looks like an electron-density histogram at a lower resolution than the original map. This is to be expected, since it is effectively obtained from the smoothed electron density. The other histograms are all symmetrical about zero, with the DDD histogram approximately Gaussian in shape and the SDD and SSD histograms increasingly more pointed. The horizontal scale of each histogram appears to be a function of grid size and resolution. This suggests that the histograms may be predicted for an unknown structure.

Wavelet-coefficient histograms of ordinary photographs have already been considered by Mallat (1989). It is at first surprising that they are so similar to the detail histograms of electron-density maps. However, this should allow us to use the mathematical model provided by Mallat to describe their shape.

5. Image construction

In order to make use of the wavelet-coefficient histograms, it was assumed that a perfect map at 10 Å resolution was already available. In addition, it was assumed that all the histograms, including that of the electron density, were also available at whatever resolution they were required. This information could then be used to increase the resolution of the starting map using the following outline.

(i) Obtain all histograms at the required resolution.

(ii) Calculate the electron density using weighted $F_{\rm obs}$ and all available phases.

(iii) Perform one stage of the wavelet transform to obtain the wavelet coefficients.

(iv) Match the wavelet coefficients to the four different histograms.

(v) Perform the inverse wavelet transform to retrieve the electron density.

(vi) Impose the space-group symmetry by averaging the density over equivalent points.

(vii) Match the electron density to its histogram.

(viii) Repeat from (iii) until converged.

(ix) Perform the Fourier transform to obtain structure factors.

(x) Compare the calculated Fs with the F_{obs} at the given resolution and estimate weights.

(xi) Repeat from (ii) until converged.

(xii) Increment the resolution and repeat from (i) until the final resolution is reached.

A flow diagram of the procedure is shown in Fig. 4. The original 10 Å phases as well as any phases obtained in previous cycles are used to calculate the electron density in (ii). As the space-group symmetry gives rise to rather complicated relationships among the wavelet coefficients which are not satisfied by the histogram matching, the calculations in (iii), (iv) and (v) are performed on the complete unit cell. The density produced in step (v) therefore lacks the correct symmetry. It is restored by averaging over equivalent points in step (vi) and then iterating the process in steps (iii) to (viii).

The weighting scheme used in step (x) is very simple. It uses the calculated Fs from step (ix) as a first approximation to the weighted F_{obs}, *i.e.* the weight $w(h) = |F_{calc}(h)|/|F_{obs}(h)|$. The weight is then increased by a small factor unless the phase is restricted by symmetry, in which case it is increased by a smaller factor, *i.e.* the amplitude of the new map coefficient is taken as

$$\begin{aligned} |F_{obs}| \quad & \text{if } (1+\varepsilon)|F_{calc}| > |F_{obs}|, \\ r(1+\varepsilon)|F_{calc}| \quad & \text{if } (1+\varepsilon)|F_{calc}| < |F_{obs}|, \end{aligned}$$

where $\varepsilon = 0.1$ for acentric data and 0.001 for centric data. The weighting scheme is at present somewhat *ad hoc* and can

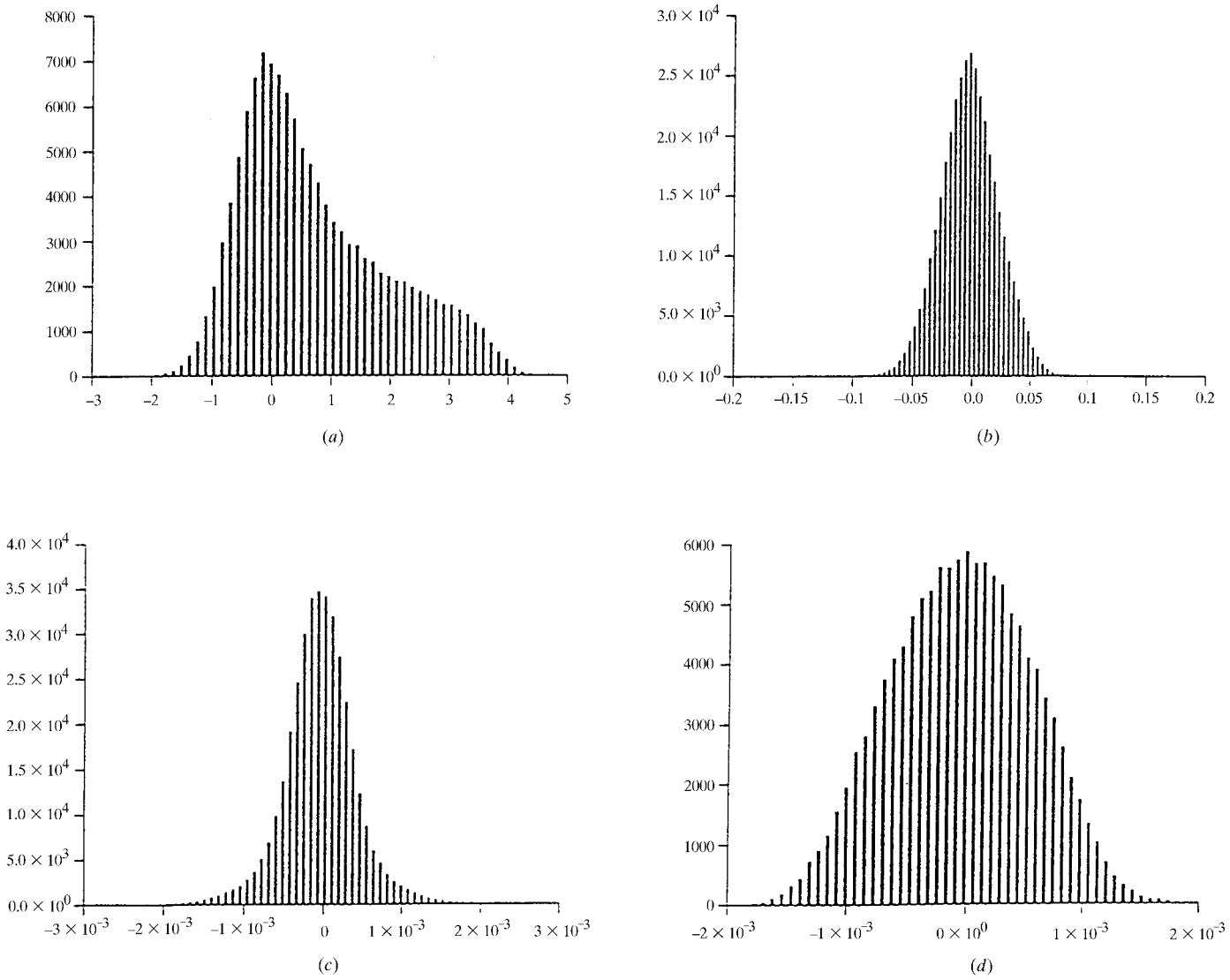

Figure 3
Wavelet-coefficient histograms: (*a*) SSS; (*b*) SSD; (*c*) SDD; (*d*) DDD.

surely be improved. So far, however, other apparently cleverer weighting schemes have all given poorer results.

6. Results

Most of the tests have been carried out on the known structure of RNAase (Sevcik *et al.*, 1981). It crystallizes with a single molecule of 96 residues in the asymmetric unit of the space group $P2_12_12_1$, with unit-cell parameters a = 64.9, b = 78.3, c = 38.8 Å and about 45% solvent content. The tests started with a perfect map at 10 Å resolution and assumed that all the wavelet-coefficient and electron-density histograms were available at any appropriate resolution. The main objective was to see if this information was sufficient to increase the resolution of the starting map.

Initially, an easier calculation was tried. Instead of using histograms of wavelet coefficients, the coefficients were calculated from an exact map of the known structure at the desired resolution. These were then sorted on value and used in the calculation as an ordered list. It was found that the resolution of the starting map could be increased as far as desired and almost without error. In practice, the phase refinement was slow, but the mean phase error could be lowered to less than 2° with sufficient cycles of refinement. However, the calculation became increasingly lengthy as the resolution increased and for this reason was stopped at about 7 Å. Although the test is unrealistic, as ordered lists of correct wavelet coefficient and electron-density values would not normally be available, it is still quite remarkable that an almost exact 7 Å map could be obtained in this way. This increase in resolution of the starting map required the calculation of 250 unique new phases.

The calculation was repeated using statistical values for the wavelet coefficients which were consistent with the correct histograms. It was quickly established that introducing too many new reflections on each increment of resolution led to poor phase determination. However, if the number of new reflections was limited to 12 or less, good phase determination could be achieved. Another device which improved the results was to apply full phase shifts only to the newest reflections and to reduce the phase shifts as a function of resolution for those reflections previously established in the calculation. This was achieved simply by averaging with the results of earlier cycles. In addition, the best results were obtained when the coarsest electron-density grid which was consistent with the resolution was used throughout the calculation. This required several changes of grid as the resolution increased. With these precautions, using calculated histograms rather than ordered lists gave a 46° weighted mean phase error over the 250 new phases – a perfectly acceptable result.

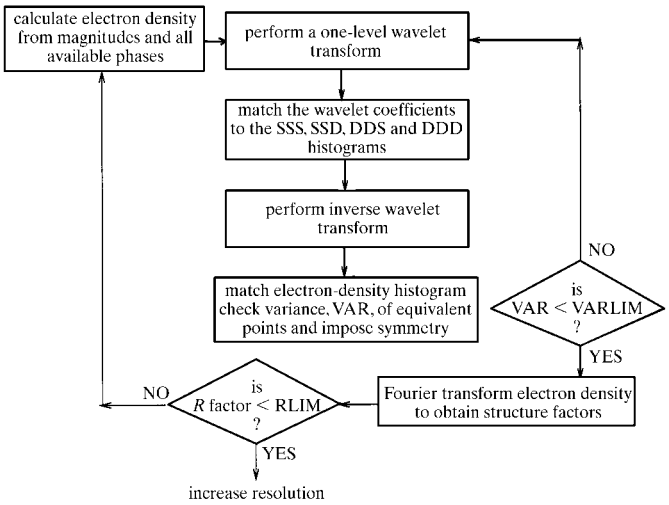

Figure 4
Flowchart of the algorithm used.

Table 1
The mean phase errors over all phases between 10 and 7 Å for the different types of wavelet coefficients used.

Wavelet coefficients used	Mean phase error (°)
All values taken from ordered lists of exact values	2
Values for SSS coefficients taken from ordered lists of exact values; statistically correct values used for all other coefficients	24
Values for DDD coefficients taken from ordered lists of exact values; statistically correct values used for all other coefficients	46
Statistically correct values used for all coefficients	46

The different wavelet histograms do not contain the same amount of information on the electron density. A series of tests was carried out in which each class of coefficient in turn was given exact values while the remainder were given statistical values consistent with the observed histograms. Exact values for the DDD coefficients gave no improvement over the use of statistical values. The greatest improvement was achieved when the SSS coefficients were given exact values. This resulted in a 24° mean phase error over the 250 new reflections. These are the coefficients which give the basic electron density upon which the detail is added and it is clearly important for this to be correct. A summary of these results is given in Table 1.

The effect of changing the wavelet function was briefly examined. All the tests described so far used Daubechies' wavelets of order 4. The program was amended to apply Daubechies' wavelet of order 6 in the hope that this more extensive wavelet would mimic a coarser electron-density grid. The results were disappointing. The new function gave rise to a larger mean phase error upon increasing the resolution of the map. This is consistent with the observation that it gave smaller magnitudes for the DDD coefficients. Clearly, other wavelet functions need to be examined.

7. Discussion

It is quite remarkable that a perfect reproduction of the image can be obtained from an ordered list of the wavelet coefficients. Even with statistical values of the coefficients, an acceptable image can still be obtained starting from a perfect

low-resolution map. Obviously, the success of this method depends upon the histograms being predictable, but it is clear from our tests that wavelet analysis has a lot to offer phase refinement and extension at low resolution. It is intended to apply this also in phase refinement at higher resolution. In the present study, the wavelets used were defined on an electron-density grid the spacing of which changes from one crystal to another. It may be more satisfactory either to perform the wavelet transform in reciprocal space or to find a wavelet function that can be scaled to match the dimensions of the crystal lattice. In addition, functions other than those of Daubechies will be investigated.

The authors are grateful to Thierry Voitot for preparing the histograms of wavelet coefficients shown in Fig. 3. The work was supported by the BBSRC Structural Biology and Design Application Initiative.

References

Collaborative Computational Project, Number 4 (1994). *Acta Cryst.* D**50**, 760–763.
Cowtan, K. D. & Main, P. (1993). *Acta Cryst.* D**49**, 148–157.
Daubechies, I. (1992). *Ten Lectures on Wavelets.* Philadelphia, PA, USA: Society for Industrial and Applied Mathematics.
Lunin, V. Yu., Urzhumtsev, A. G. & Skovoroda, T. P. (1990). *Acta Cryst.* A**46**, 540–544.
Mallat, S. G. (1989). *IEEE Trans. Pattern Anal. Mach. Intell.* **11**, 674–693.
Press, W. H., Teukolsky, S. A., Vetterling, W. T. & Flannery, B. P. (1992). In *Numerical Recipes in Fortran*, 2nd ed. Cambridge University Press.
Sevcik, J., Both, V., Halicky, P. & Zelinka, J. (1981). *Biologia*, **36**, 235–239.
Strang, G. & Nguyen, T. (1996). *Wavelets and Filter Banks.* Wellesley, MA, USA: Wellesley–Cambridge Press.
Zhang, K. Y.-J. & Main, P. (1990). *Acta Cryst.* A**46**, 41–46.